HHS Public Access

Author manuscript

Hepatology. Author manuscript; available in PMC 2021 January 01.

Published in final edited form as:

Hepatology. 2020 January ; 71(1): 14–30. doi:10.1002/hep.30815.

Analysis of host responses to hepatitis B and delta viral infections in a micro-scalable hepatic co-culture system

Benjamin Y. Winer[1], **Jenna M. Gaska**[1], **Gabriel Lipkowitz**[1], **Yaron Bram**[4], **Amit Parekh**[2], **Lance Parsons**[3], **Robert Leach**[3], **Rohit Jindal**[2], **Cheul H. Cho**[2], **Anil Shrirao**[2], **Eric Novik**[2], **Robert E. Schwartz**[4], **Alexander Ploss**[1,5]

[1]Department of Molecular Biology, Princeton University, Princeton, NJ 08544, USA

[2]Hurel® Corporation, North Brunswick, NJ 08902, USA

[3]Lewis-Sigler Institute for Integrative Genomics, Princeton University, Princeton, NJ 08544, USA

[4]Division of Gastroenterology & Hepatology, Department of Medicine, Weill Medical College of Cornell University, New York, NY 10021, USA

Abstract

Hepatitis B virus (HBV) remains a major global health problem with 257 million chronically infected individuals worldwide, of whom approximately 20 million are co-infected with hepatitis delta virus (HDV). Progress towards a better understanding of the complex interplay between these two viruses and development of novel therapies have been hampered by the scarcity of suitable cell culture models that mimic the natural environment of the liver. Here, we established HBV and HBV/HDV co- and super-infections in self-assembling co-cultured primary human hepatocytes (SACC-PHHs) for up to 28 days in a 384 well format and highlight the suitability of this platform for high-throughput drug testing. We performed RNAseq at days 8 and 28 on SACC-PHHs either HBV mono- or HBV/HDV co-infected. Our transcriptomic analysis demonstrates that hepatocytes in SACC-PHHs maintain a mature hepatic phenotype over time regardless of infection condition. We confirm that HBV is a stealth virus as it does not induce a strong innate immune response; rather oxidative phosphorylation and extracellular matrix-receptor interactions are dysregulated to create an environment that promotes persistence. Notably, HDV co-infection also did not lead to statistically significant transcriptional changes across multiple donors and

[5]Correspondence should be addressed to A.P. (aploss@princeton.edu).

Author contributions

B.Y.W., J.M.G. and A.P. designed and performed experiments and wrote the manuscript. G.L., Y.B., R.J., Am. P., C.C., and A.S. performed experiments. L.P. and R.B. analyzed data and edited the manuscript. R.E.S edited the manuscript. E.N. performed experiments and edited the manuscript.

Data availability. The data that support the findings of this study are available from the corresponding author upon request. All code in R along with outputs (i.e. tables of differential gene expression) can be accessed at https://github.com/aploss/SACC-PHH-RNASeq. The RNASeq data generated in this study are deposited in the NCBI Gene Expression Omnibus (GEO) database (accession number GSE112118). For reviewer-only access, please use the token szmjswysvhaltep. This data will be made publicly accessible upon manuscript acceptance.

Supplementary data: The supplementary materials document contains a detailed materials and methods section as well as all supplementary figures.

Conflicts of Interest.

The following authors declare competing financial interests. R.J., Am.P., C.C., A.S. are employees of the Hurel Corporation of which E.N. is also a stockholder. A.P. is a member of the Scientific Advisory Board of the Hurel Corporation. B.Y.W., J.M.G., Y.B., R.E.S., G.E.L., L.P., and R.L. do not have any conflicts of interest.

replicates. The lack of innate immune activation is not due to SACC-PHHs being impaired in their ability to induce interferon stimulated genes (ISGs). Rather poly(I:C) exposure activates ISGs and that this stimulation significantly inhibits HBV infection but only minimally affects the ability of HDV to infect and persist. Altogether, these data demonstrate that the SACC-PHH system is a versatile platform for studying HBV/HDV co-infections and holds promise for performing chemical library screens and improving our understanding the host response to such infections.

Keywords

Hepatitis B virus; hepatitis delta virus; viral hepatitis; primary hepatocyte culture; tissue engineering; innate immunity; RNAseq; transcriptomic; host response

Introduction

Hepatitis B virus (HBV), which is part of the *Hepadnaviridae* family, has a compact 3.2 kilobase relaxed circular DNA (rcDNA) genome encoding four viral gene products: the viral polymerase, which also acts as a reverse transcriptase; the core protein (HBcAg), which forms the nucleocapsid; the X gene (HBx), which is thought to epigenetically regulate HBV covalently closed circular DNA (cccDNA); and the large (L), medium (M), and small (S) envelope proteins (HBsAgs) (1). HBV is considered a uniquely hepatotropic virus, entering its target cells, human hepatocytes (PHHs), by utilizing the bile acid transporter human sodium-taurocholate co-transporting polypeptide (hNTCP) (2). The HBV rcDNA enters the nucleus where it is repaired via host cell machinery to form cccDNA, the stable and persistent form of the HBV genome (1).

A satellite virus of HBV and sole member of the *Deltavirus* genus, the enveloped hepatitis delta virus (HDV) has a 1679-nucleotide, negative-sense RNA genome encoding for two isoforms of the delta antigen (HDAg) (3). HDV highjacks the HBsAgs (L, M, and S) for packaging infectious HDV virions and thus relies upon co-infection with HBV (3). Consequently, HDV also utilizes hNTCP as a receptor but replicates its genome independent of HBV.

In addition to a very limited tissue tropism, HBV and HDV exhibit a restricted host tropism, robustly infecting only human and chimpanzee hepatocytes (4). However, HDV infection has been experimentally established in species susceptible to other hepadnaviruses related to HBV, such as woodchuck hepatitis virus (WHV) in woodchucks. Recently, HDV-like viruses have also been detected in birds and snakes (5, 6). However, these viruses significantly differ from human HDV in their cellular tropism and genomic sequence. Studying these two viruses has thus historically been difficult. Transfections of plasmids encoding HBV over-length genomes have been used to analyze aspects of viral replication and gene transcription in human hepatoma cells (7). However, the artificial nature of such systems fails to fully recapitulate the mechanisms observed under native infection conditions. The cell line HepaRG, derived from a hepatocellular carcinoma (HCC) biopsy, is susceptible to HBV infection (8) but only after prolonged re-differentiation, limiting its utility. With the discovery of hNTCP as a bona fide receptor for HBV and HDV, ectopic expression of this protein subsequently made human hepatoma cell lines, such as HepG2 and Huh7,

susceptible to both HBV and HDV infection (2, 9). Although low-cost and easy to culture, hepatoma lines remain less than ideal due to their abnormal proliferation and aberrant gene expression profiles as compared to PHHs.

Previous studies have shown that PHHs and fetal human hepatocytes are susceptible to infection with HBV and other hepatotropic viruses (10-12). However, monoculture PHHs rapidly de-differentiate following plating, with concomitant loss of susceptibility to HBV limiting any analysis to a few days. This de-differentiation can be delayed by co-culturing with non-parenchymal cells (13, 14). In both self-assembling co-cultures of PHHs (SACC-PHHs) and micropatterned co-cultures (MPCCs), PHHs are stabilized, maintaining a phenotype similar to hepatocytes in the 3D context of the liver. MPCCs of PHHs are susceptible to a variety of liver-tropic pathogens (15, 16). However, HBV infections of MPCCs, which persisted only up to 16–19 days, required pre-selection of susceptible donors, (17). The requirement for JAK/STAT inhibition consequently reduces this platform's suitability for thoroughly investigating host-virus interactions. A recent publication on a 3D microfluidics PHH system established infection for up to 40 days in a 12 well format (18), but this system is not easily scalable and requires advanced technical skills to operate.

Recently, we showed that SACC-PHHs can be robustly and persistently infected with HBV for up to 40 days with little donor-to-donor variability and without suppressing innate immune signaling (19). Building on this work, we demonstrate here that PHHs in SACCs support long-term HBV-HDV co-infection in microwell plate formats. To our knowledge, establishing long-term HBV/HDV infection in a microscale, 384 well format has not previously been reported. It is a significant improvement even over 96 well formats as it would enable high-throughput screens in automated settings. We further utilized this model to probe the host responses to both viruses, and we confirm that HBV is a "stealth virus." Going beyond this, we interrogated the role of innate immune activation on HBV and HBV/HDV viral persistence, giving insight into viral dynamics and the clinical significance of innate immune recognition. Our work demonstrates the versatility of the SACC-PHH platform for modeling complex liver diseases, such as HBV, HBV/HDV and potentially other clinically relevant liver infections, in a controlled experimental setting.

Methods

For full experimental details please see the materials and methods section in the Supplemental Materials document.

Generation of self-assembling primary hepatocyte co-cultures (SACC-PHHs)

Cryopreserved human hepatocytes were obtained from Bioreclamation IVT Inc. (Westbury, NY), ThermoFisher Scientific (Waltham, MA), Sekisui Xenotech LLC (Kansas City, KS), and Corning Inc (Corning, NY). The co-culture model consists of a mixture of human hepatocytes and non-parenchymal mouse embryonic fibroblast 3T3-J2 cells (CCL-92, ATCC, Manassas, VA)(14, 20). All co-cultures were plated on collagen type-I coated, tissue culture treated plates 96 well and 24 well (Corning Inc, Corning NY).

RT-qPCR of ISGs OAS1, MX1, and ISG15

To quantify fold changes of OAS1, MX1, and ISG15 levels in SACC-PHHs total RNA was isolated from lysed cells using an EZ-10 Spin Column Total RNA Miniprep Super Kit (BioBasics, New York City, NY). A mastermix for each gene to be quantified was made following the Luna® Universal One-Step RT-qPCR Kit (New England Biolabs, Ipswitch, MA) protocol with forward and reverse primers at a 3 μM final concentration (see supplemental materials for primer sequences). The plate was centrifuged at 3,000 rpm for 1 min. The following PCR program was run on a Step One Plus qPCR machine (Life Technologies, Carlsbad, CA): 50°C for 10 min, 95°C for 1 min, followed by 40 cycles of 95°C for 15 sec, 60°C for 1 min, followed by a melt curve of 95°C for 5 sec, 65°C for 5 sec, 95°C for 5 sec and 50°C for 5 sec.

Statistical analysis

Statistical analysis was performed using GraphPad Prism Software (GraphPad, La Jolla, CA). A one-way analysis of variance (ANOVA) using Bonferroni parameters was used. P values less than 0.05 were considered statistically significant.

Results

Infection of SACC-PHH with HBV does not require DMSO but is significantly enhanced by PEG.

To facilitate robust HBV infection in both human hepatoma cells overexpressing hNTCP as well as in PHH monocultures, polyethylene glycol (PEG) and dimethyl sulfoxide (DMSO) are routinely added during infection (21). Optimal DMSO concentrations used for HBV infection and maintenance in hepatoma cells and PHHs vary from 1–2.5% by volume. We titrated the DMSO concentration in our SACC-PHHs (0–2% v/v). At 0.5% DMSO, no statistically significant difference was observed in the activity of CYP2C9 and CYP3A4, hepatic proteins important for drug metabolism (Supporting Fig. 1). SACC-PHHs were challenged with HBV +/− PEG and DMSO. HBV infection was established when PEG was present at the time of challenge, regardless of pre-treatment with or maintenance in DMSO (Supporting Fig. 2 and 3). However, upon omission of PEG during HBV challenge, viral persistence was only observed in cultures maintained in DMSO. Therefore, although DMSO was not essential for productive HBV infection when PEG was present, removal of PEG resulted in a greater need for DMSO treatment (Supporting Fig. 2D–G, Supporting Fig. 4A and 4B). Infection rates were further improved when both additives were present. (**Please see** extended results section in the supporting material **for more details**)

SACC-PHHs support HBV/HDV co- and super-infection.

Previous work demonstrated that PHHs are susceptible to HDV virions enveloped with proteins from the related hepadnavirus WHV (22). However, there is limited information on HBV/HDV co- or super-infection in cultured PHHs, and thus we sought to characterize viral dynamics during such infections in SACC-PHHs. Cultures were challenged with either HBV alone, co-infected with HBV/HDV, or super-infected with HDV once HBV persistence was established for 10 days. Irrespective of the donor used (see Table 1 and 2 for donor details),

PHHs became robustly infected with HBV during mono-infection, reaching 2.5–3 Au of HBsAg in culture supernatants (Fig. 1A). Infection was further corroborated by 100–1,000 times higher HBV DNA levels (Fig. 1C, Supporting Fig. 5A) and about 10,000 times higher HBV pgRNA levels (Fig. 1D, Supporting Fig. 4B) in the cell lysates of HBV-challenged versus mock-infected cells. Regardless of co- or super-infection, levels of HBsAg exceeded 3 Au in the supernatants of all donor cultures (Fig. 1A). SACC-PHH cultures became HDV viremic during both co- and super-infections as evidenced by a ca. 1,000-fold increase of HDV RNA from pre-challenge levels in the culture supernatants (Fig. 1B, Supporting Fig. 4C).

Differences in HBV replication intermediates were observed across infection conditions, with ~0.5 log higher levels of HBV DNA in HBV mono-infected cultures as compared to HBV/HDV super-infected cultures (Fig. 1C). Although there was no significant difference in HBV DNA levels between mono- and co-infected cultures at day 8, there was a significant reduction by day 28 in super- versus mono-infected cultures (Fig. 1C). HBV pgRNA levels, however, were 10-fold higher in co-infected SACC-PHH lysates than those of super-infected cells (Fig. 1D). Of interest, the level of HDV genomic RNA was about 10-fold higher in the cell lysates of HBV/HDV co-infected samples compared to super-infected samples (Fig. 1E). The observed differences in viral replication intermediates were not attributable to culture deterioration as human albumin (hAlb) levels were similar across groups (Supporting Fig. 6).

Determination of number of HBV, HDV, and co-infected SACC-PHHs

To determine the infection rate, we challenged SACC-PHHs with either HBV, HDV, HBV/HDV, or no virus. At 8 and 28 days post infection (dpi) cells were fixed and stained for nuclei, HBcAg and HDV genomic RNA using a viral proximity ligation assay for RNA and tyramide signal amplification (vPLAYR/TSA) (Fig. 2A, Supporting Fig. 7). We have used the vPLAYR/TSA technique previously to determine the frequency of HDV viral infected cells in liver tissue from 1.3xHBV/hNTCP-BAC tg NRG mice (23). vPLAYR/TSA is a highly sensitive technique developed and used to directly detect small RNA fragments (24). The percent of infected cells across multiple frames (~800 cells over three frames) was then quantified for each condition (Fig. 2B–D). For HBV mono-infected cells, ~30–45% of cells were HBcAg+ at either time point. However, dual positive frequencies in HBV/HDV co-infected cells were 29–36% at 8 dpi and 15–28% at 28 dpi. When detecting HDV genomic RNA-positive cells, HDV mono-infected SACC-PHHs had 60–85% of cells infected on day 8 but this was slightly reduced to 42–52% by day 28. These data show collectively that there are a large fraction of cells infected with HBV and/or HDV. HDV RNA was readily detectable in supernatant of HBV/HDV co-infected cultures (Supporting Fig. 8), providing further evidence for bona fide HDV replication.

Characterization of HBV infection in a microscale 384 well format.

To further increase the utility of our platform for high-throughput screening (HTS), we scaled the SACC-PHH cultures down to a 384-well format. In this micro-format, SACC-PHHs remained susceptible to HBV infection as seen by greater than 3 Au HBsAg in the supernatants and only 3.12% variation across all 384 wells following challenge with cell

culture-produced HBV (HBVcc) (Fig. 3A–B). This was corroborated by 2.5 logs higher levels of HBV DNA (Fig. 3C) and 4 logs higher HBV pgRNA (Fig. 3D) in the cell lysates of HBV-challenged versus mock-infected SACC-PHHs.

Assessment of clinically relevant drug candidates for HBV mono- and HBV/HDV co-infections.

In this micro-format, we then tested the prophylactic and therapeutic effects of clinically relevant DAAs on either HBV mono- or HBV/HDV co-infections. In SACC-PHHs, prophylactic entecavir (ETV) treatment reduced HBV DNA levels in a titration-dependent manner by ~99% at a concentration of 250 nM to ~40% at a concentration of 16 nM (Fig. 3E). When persistently HBV-infected SACC-PHHs were treated with ETV, a similar titration-dependent reduction in HBV DNA levels was observed, from ~95% at 250 nM to ~50% at 16 nM (Fig. 3E).

Recently, the HBV/HDV entry inhibitor Myrcludex B (MyrB) was shown to suppress both HBV DNA and HDV RNA in co-infected patients (25). SACC-PHHs plated in the 384 well format were either pre-incubated with MyrB or a control peptide (19) prior to HBV infection or MyrB was administered therapeutically. In agreement with previous studies, MyrB effectively blocked ~99% of HBV at a concentration of 1000 nM, 95% at 100 nM and ~80–85% at 10 nM relative to treatment with the control peptide (Fig. 3E). Moreover, when persistent HBV infections were first established and SACC-PHHs therapeutically treated with MyrB, infection was reduced by ~97% at 1000 nM and 50% at 10 nM (Fig. 3E).

We next extended the analysis to treatment of HBV/HDV co-infected cultures in 384-well plates. Upon challenge with HBV/HDV, HDV RNA levels in the supernatant were 500-fold higher compared to the control (Supporting Fig. 9A). HDV genomic RNA levels in cell lysates were 3–3.5 logs higher than mock wells (Supporting Fig. 9B). In addition, high levels of HBsAg, between 0.8–1 Au, were observed for co-infected samples (Supporting Fig. 9C). Together, these data indicate that SACC-PHHs can be successfully co-infected with HBV/HDV in this microwell format.

Next, we aimed to ascertain the effect of ETV on HDV in HBV/HDV co-infected SACC-PHHs. Prophylactic ETV treatment resulted in a dose dependent inhibitory effect, with an ~80% reduction in HDV RNA levels in the supernatant at 250 nM to a 45% reduction at 16 nM relative to control (Fig. 3F). Therapeutic ETV treatment was less effective, with ~70% inhibition at 250 nM to only 20% at 64 nM. These effects are presumably due to the inhibition of HBV replication at these doses. The effect of ETV at 32 and 16 nM was minimal. Prophylactic MyrB treatment reduced HDV RNA levels by ~87% at 1000 nM and ~70% at 10 nM (Fig. 3F) while therapeutic treatment resulted in ~60% or 15% reduction in HDV RNA levels at 1000 nM or 10 nM, respectively (Fig. 3F). Notably, no major differences in hAlb levels were observed for HBV mono- or HBV/HDV co-infected samples, regardless of treatment (Supporting Fig. 10).

Characterization of transcriptional changes occurring in HBV mono- and HBV/HDV co-infected SACC-PHHs at early and late stages of infection.

The transcriptional changes that occur in PHHs upon HBV mono- or HBV/HDV co-infection remain incompletely characterized due to rapid de-differentiation and subsequent loss of infection in traditional PHH culture systems. With our platform's improved ability to maintain persistent mono- or co-infection for up to 28 days, we sought to characterize the host response to viral infection at both early (8 dpi) and late (28 dpi) timepoints. We compared the cellular transcriptome by using RNA sequencing (RNASeq) of control, HBV mono-, and HBV/HDV co-infected SACC-PHH cell from donors HU1007, HU1016, HU1019 and HU1020 as they had similar viral kinetic profiles (Fig. 1). Principal component analyses and heat maps of sample-sample distances based off the regularized $\log_2$-transformed (rlog) counts (routinely used to decrease the variance across samples for genes with low counts) for human and HBV genes demonstrated that variability between samples was due more to variability between donors and not infection, as samples from the same donor generally clustered together regardless of infection status (Supporting Fig. 11–12).

We also used our RNASeq data to confirm our SACC-PHH platform's faithful recapitulation of the liver-specific transcriptional profile observed in PHHs within the 3D context of the liver. We utilized a previously generated list of drug-metabolizing enzymes, predominantly regulated at the transcriptional level and expressed in the human liver, that has been used to evaluate the hepatic phenotype of human ectopic artificial livers as well as fetal hepatocytes and hepatocyte-like cells (HLCs) (26). We assessed rlog counts for this panel of genes in each of our samples and found they remained largely unchanged independent of donor, time or infection (Fig. 4).

We then assessed the differential gene expression between infection conditions after accounting for donor variation. Compared to mock-infected controls, HBV mono-infected and HBV/HDV co-infected SACC-PHHs had more differentially expressed genes ($p_{adj} \leq 0.05$ and absolute value($\log_2$(fold change)) ≥ 0.5) at 8 dpi (mono-infected, 90 genes; co-infected, 53 genes) versus 28 dpi (mono-infected, 0 genes; co-infected, 3 genes) (Fig. 5A–B). For both mono- and co-infections compared to mock, more genes were downregulated, but all four HBV genes were consistently upregulated at both time points (Fig. 5A), with normalized counts of HBsAg and viral polymerase were higher than those of HBx and core across all infected samples (Supporting Fig. 13). Besides the viral genes, four other genes were downregulated in both acutely and chronically HBV/HDV co-infected SACC-PHHs compared to mock cultures: platelet and endothelial cell adhesion molecule 1 (PECAM1), deoxyribonuclease 1 like 3 (DNASE1L3), cadherin 5 (CDH5), and phosphatase domain containing paladin 1 (PALD1). When examining the co- versus mono-infected samples, seven genes were downregulated at both 8 and 28 dpi: ficolin 3 (FCN3), DNASE1L3, CDH5, roundabout guidance receptor 4 (ROBO4), PECAM1, kinase insert domain receptor (KDR) and CD93.

Among the differentially expressed genes of HBV mono-infected versus mock SACC-PHHs, the pathways oxidative phosphorylation and ECM-receptor interactions were enriched at 8 dpi (padj ≥ 0.07; Fig. 5C). When comparing differentially expressed genes in the co- to mono-infected samples, three additional pathways – ribosome, focal adhesion, and

protein digestion and absorption – were significantly enriched at 8 dpi. Only the ribosome pathway was still significantly enriched at 28 dpi. No pathways were enriched for the co-infected samples relative to mock, and significant enrichment of innate immune pathways was not observed under any condition. In contrast, by gene ontology (GO)-term analysis, there was significant enrichment (q.val ≥ 0.05) amongst upregulated genes for members of "type I IFN signaling pathway" at 8 dpi for HBV mono-infected samples compared to mock (Supporting Fig. 14). When comparing differential gene expression from 8 to 28 dpi for each infection condition, only some metabolism pathways were uniquely enriched in the HBV mono-infected samples, along with complement and coagulation cascades and cell adhesion molecules (Supporting Fig. 15). Other metabolism and biosynthesis pathways were consistently enriched across all infection conditions. Minimal transcriptional changes occurred in the murine non-parenchymal stromal cells across all conditions tested (Supporting Fig. 16). Having observed from our transcriptional analysis that HBV/HDV co-infection did not induce strong innate immune activation, we compared OAS-1 and ISG15 induction by RT-qPCR across these donors plus donor HU1003, which had shown very different viral kinetics (Figure 1, middle). We observed that OAS-1 was consistently not induced in any donor under any condition. However, ISG15 was induced in HU1003 SACC-PHHs at 8 dpi (Supporting Fig. 17 A–B). In corroboration of our RNASeq analysis, RT-qPCR of our RNASeq samples showed little change in the average expression of MX1 and (Supporting Fig. 18A) a marked decrease in CDH5 at 8 dpi in the co-infected samples (Supporting Fig. 18B).

HBV/HDV co-infection does not disrupt innate immune activation by polyinosinic:polycytidylic acid (poly(I:C))

As we observed no enrichment of innate immune pathways but did observe enrichment of members of the GO term "type I IFN signaling pathway" amongst upregulated genes in HBV versus mock infected samples at 8 dpi, we wanted to confirm that our SACC-PHHs were competent for ISG expression. As such, poly(I:C), a double-stranded RNA mimic that is a strong inducer of cell-intrinsic innate immune responses, was transfected into SACC-PHHs (Fig. 6A), resulting in induction of OAS-1 (Fig. 6B, left), MX1 (Fig. 6B, middle) and ISG15 (Fig. 6B, right). Next, we aimed to determine whether an established co-infection with HBV/HDV would prevent innate immune activation by poly(I:C) and thus we transfected poly(I:C) into cells persistently co-infected with HBV/HDV for 12 days (Fig. 6A). Innate immunity activation upon poly(I:C) transfection was not inhibited by the established HBV/HDV infection; rather, we observed increases in relative OAS-1 (Fig. 6C, left), MX1 (Fig. 6C, middle), and ISG15 (Fig. 6C, right) expression in cell lysates at 12 dpi/12 *hours* post-poly(I:C) transfection. Thus, in contrast to other viruses, the lack of antiviral innate immune signatures during HBV/HDV co-infection cannot be attributed to a generalized suppression of innate immune pathways.

Characterization of HBV viral kinetics and innate immune activation upon poly(I:C) transfection.

We then tested if inducing these responses inhibited HBV mono-infection, challenging our SACC-PHHs either (i) with HBV; (ii) pre-treating with poly(I:C); or (iii) first infecting with HBV and then transfecting in poly(I:C) at 12 dpi (see schematic in Fig. 7A). Once more,

untreated SACC-PHHs were readily infected with HBV, exhibiting high levels of HBsAg in the supernatants (Fig. 7B and 7C). However, cells treated with poly(I:C) prior to infection demonstrated HBsAg levels 0.5–0.7 Au lower than non-poly(I:C)-treated samples (Fig. 7B and 7C, Supporting Fig. 19A and C). SACC-PHHs already persistently infected with HBV for 12 days and then treated with poly(I:C) showed a decline of 0.5–0.8 Au in HBsAg levels over the subsequent 10 days (Fig. 7B and 7C, Supporting Fig. 19A and C). This suggests that in our SACC-PHHs, induction of cell-intrinsic innate immune responses can inhibit HBV infection.

Characterization of HBV/HDV viral kinetics and innate immune activation upon poly(I:C) transfection

Pegylated interferon is the only currently approved treatment for HBV/HDV co-infected patients and has debatable efficacy. We next wanted to test if inducing innate immunity inhibited co-infections, challenging our SACC-PHHs either (i) with HBV/HDV; (ii) pre-treating with poly(I:C) and then co-infecting; or (iii) first co-infecting and then transfecting in poly(I:C) at 12 dpi (see schematic in Fig. 8A). Upon co-infection, high levels of HBsAg were observed (Fig. 8B and 8C), but pre-treatment or treatment 12 dpi with poly(I:C) dampened HBsAg levels in the supernatants (Fig. 8B and 8C, Supporting Fig. 19B and D). This suggests that co-infection with HDV does not antagonize the innate immune response initiated by poly(I:C). In co-infected, non-poly(I:C)-treated samples, intracellular HDV genomic RNA levels were high (1×10^5 genome equivalents (GE)/well) at both 12 and 22 dpi (Fig. 8D, left). In contrast, intracellular HDV genomic RNA was ~1 log lower 12 hours post poly(I:C) transfection (Fig. 8D, middle) but by 22 dpi was comparable to the non-poly(I:C)-treated controls. Notably, pre-treatment with poly(I:C) resulted in ~1 log lower levels of intracellular HDV genomic RNA at both 12 and 22 dpi (Fig. 8D, **right**).

Discussion

Historically, there have been several impediments to successfully utilizing PHH culture systems for the investigation of HBV mono- and HBV/HDV co-infections. Additives such as DMSO and PEG are relied upon to achieve robust infection. In SACC-PHHs robust HBV mono- or HBV/HDV co-infection can be achieved with pre-treatment and maintenance with 0.5% DMSO without perturbing the PHH gene expression profile. Although PEG can also be removed from the viral challenge conditions, its presence did greatly enhance the infection in SACC-PHHs.

The rapid de-differentiation of PHHs has been a second difficulty in generating advanced PHH culturing systems that can support persistent infections. We aimed to establish HBV/HDV co-infection in our SACC-PHHs. In patients, acute hepatitis D is mostly caused by HBV/HDV co-infection and resembles an acute HBV mono-infection in adults, with less than 5% becoming chronic (27). However, superinfection, whereby a chronic HBV patient is infected with HDV, results in more severe acute hepatitis that leads to chronicity in up to 80% of individuals (28). During co-infection, high serum levels of both HBV DNA and HDV RNA are observed. However, during superinfection, HBV levels are suppressed (28). Similar to co-infected patients, the supernatants of our co-infected SACC-PHH cultures

contained high levels of both HBsAg and HDV RNA over the course of infection whereas superinfected SACC-PHHs exhibited reduced HBsAg levels that rebounded by 18 days post HDV infection and 10-fold lower HBV DNA by 28 dpi, indicating HBV suppression. These data suggest SACC-PHHs can recapitulate the infection kinetics observed in both acute and chronic HBV and HBV/HDV infected patients.

We observed high levels of infection in HBV-challenged cells (36–50% HBcAg+),between 40–80% HDV mono-infection, and ~15–38% dual infected cells in HBV/HDV co-infected SACC-PHHs. HDV mono-infection rates in mono-cultured PHH's have been previously reported at the high end with 37–40% (29). We utilized a vPLAYR/TSA procedure which allowed for sensitive detection of HDV genomic RNA. Of interest, we observed a range of signal intensities within the infected cell population, possibly indicating heterogeneity in the levels of HDV replication across the cell population.

We successfully scaled the SACC-PHH platform to 384 wells and demonstrated persistent mono- or co-infection for up to 28 days. Of note, susceptibility was not donor-dependent as all donors tested supported persistent infection. We validated our platform for HTS by testing the efficacy of drugs in clinical trials for treating HBV and HDV, observing in the 384 well format the same inhibitory effects seen in patients.

Lastly, it has been unclear how well cultured PHHs resemble those in the 3D context of the liver at the transcriptomic level. Here, we demonstrated that regardless of time, donor or infection, a majority of liver-specific transcripts commonly used as markers of a hepatic phenotype remained upregulated in our SACC-PHHs, arguing that the differential gene expression profiles derived from these samples were a result of infection, not culture deterioration. Furthermore, the non-parenchymal cells co-cultured with our PHHs demonstrated little differential transcriptional activity in infected versus non-infected cultures, suggesting minimal impact on infection. Regardless of timepoint, HBV viral genes remained highly upregulated in both mono- and co-infected samples, corroborating the persistence of infection. Of note, HBsAg was the most upregulated HBV transcript and HBx the least upregulated across all experimental conditions.

The host response to HBV mono- and HBV/HDV co-infection has been a contentious area of research, especially regarding innate immunity. While some studies have observed innate immune activation upon infection (30), others have reported minimal to none, leading to the characterization of HBV as a "stealth" virus (31). For HBV to evade inducing an innate immune response, it must either never be detected or inhibit activation. Recently, it was observed that liver biopsies freshly isolated from chronic HBV patients did not have an induced IFN or ISG response unless poly(I:C) was transfected into cells (32), suggesting HBV evades detection. In the SACC-PHH platform, the majority of changes in gene expression relative to mock occurred at day 8 post infection. However, only the HBV mono-infected samples at 8 dpi exhibited coordinated changes of genes involved with pathways such as oxidative phosphorylation and ECM-receptor interaction, confirming other studies that have suggested HBV hijacks the host machinery to promote viral production and persistence (33). The lack of enrichment for pathways in the co-infected versus mock samples was not surprising given the lower level of differential gene expression. Although

we tested multiple donors in multiple replicates for this study, we still cannot be certain that additional samples might not lead to a greater differential.

In this study, we did not observe significant pathway enrichment for innate immune activation in response to HBV mono-infection. Only at 8 dpi did we see amongst upregulated genes enrichment for the GO term “type I IFN signaling pathway.” At best, this indicates a weak innate immune response, potentially disjointed in its manifestation since we did not detect coordinated changes in other related pathways or GO terms. Similarly, we did not observe innate immune activation in HBV/HDV co-infected samples. This is in contrast to data that showed HDV elicited a ~1.5 log peak induction of IFN β and λ expression at 5 dpi and a decrease by 7 dpi in mono-cultured PHHs (29). However, there are several factors that make the comparison of this study to the present one questionable, including cell type (HepaRG and hNTCP-expressing HepG2 cells versus PHHs), type of infection (HDV mono-infection versus our co-infections), and variable timepoints (3–7 dpi versus 8 and 28 dpi in our study). Importantly, the “early” and “late” time points were unattainable in previous studies as PHH cultures could not be maintained for long periods of time, only allowing for a short window of investigation. However, more broadly the unbiased approach to investigating the transcriptome of infected PHHs shows how our platform can be utilized to probe virus-host interactions to gain a better understanding of the changes occurring within infected human hepatocytes that promote establishment and persistence.

We also corroborated that the lack of a robust innate immune response to mono- or co-infection in our transcriptomic data is biologically relevant and not merely a consequence of our co-culture platform. Our data suggest that HBV is likely undetected by host immune pathways as triggering ISG induction by poly(I:C) transfection led to a significant reduction in HBV viral parameters, indicating the virus remains sensitive to innate immune responses. It is feasible that HBV may not be able to overcome a strong coordinated innate immune response as induced by poly(I:C). If a weak or deficient innate immune response is triggered upon HBV infection, the virus might still be able to evade or modulate the host response. Additionally, we observed that there is undeniably a genetic component to the differences in observed response depending on the donor used. For example, one donor (HU1003), although readily susceptible to HBV and HBV/HDV co-infection, had markedly different viral kinetics compared to the donors used for RNASeq and, unlike these other donors, exhibited upregulated levels of ISG15 8 dpi. It will be of interest in future work to utilize larger panels of donors classified into subgroups by their viral kinetics to assess possible connections between their transcriptomic and infection profiles.

The SACC-PHH platform has several advantages over current systems, including improved infection conditions, scalability to a 384-well format enhancing utility for HTS or large-scale genetic screens. Both a benefit and a drawback is that the SACC-PHH system is comprised of only permissive PHHs and non-permissive non-parenchymal stromal cells. Thus, innate/cell-intrinsic immune activation is decoupled from the adaptive immune response. Co-culturing SACC-PHHs with other nonparenchymal and/or immune cells, such as $CD8^+$ T cells, would be a further advance of this system that could aid in our understanding of T cell exhaustion and HBV pathology. Lastly, the RNASeq data set

described here is a novel resource to begin understanding the global effects, or lack thereof, that occur during the early and late stages of infection in PHHs.

Supplementary Material

Refer to Web version on PubMed Central for supplementary material.

Acknowledegements

We would like to thank Stephanie Oh and members of the Ploss lab, in particular Elham Shirvani-Dastgerdi and Lei Wei, for critical discussion and edits on the manuscript. We thank Gary Laevsky and the Nikon Center of Excellence for generous assistance with imaging. We thank Matthew Cahn (Princeton University) for his assistance in facilitating the submission of our raw and processed data to GEO. HepG2.2.15 cells were kindly provided by Christoph Seeger (Fox Chase Cancer Center). The pSVL(D3) was a kind gift from John Taylor. (DFHS18PPC002) and Myrcludex B was gifted by Stephan Urban, University of Heidelberg.

Financial support:

This study is supported in part by grants from the National Institutes of Health (R01AI079031, R01AI107301, R21AI117213, all to AP), a Burroughs Wellcome Fund Award (1015389) for Investigators in Pathogenesis (to AP) and funds from Princeton University (to AP). R.E.S. is supported by grants (1K08DK101754 and 1R03DK117252) from the NIDDK as well as a (1R21AI117213) from the NIAID. B.Y.W. is a recipient of a F31 NIH/NRSA Ruth L. Kirschstein Predoctoral fellowship (1F31AI122480-01A1) awarded from the NIAID and a predoctoral fellowship from the New Jersey Commission on Cancer Research.

Abbreviations:

(HBV)	Hepatitis B virus
(HDV)	hepatitis delta virus
(PHHs)	primary human hepatocytes
(SACC-PHHs)	self-assembling co-cultured primary human hepatocytes
(DMSO)	dimethyl sulfoxide
(PEG)	polyethylene glycol
(poly(I:C))	polyinosinic:polycytidylic acid

References:

1. Seeger C, Mason WS. HBV replication, pathobiology and therapy: Unanswered questions. J Hepatol 2016;64:S1–S3. [PubMed: 27084030]
2. Yan H, Zhong G, Xu G, He W, Jing Z, Gao Z, Huang Y, et al. Sodium taurocholate cotransporting polypeptide is a functional receptor for human hepatitis B and D virus. Elife 2012;1:e00049.
3. Lempp FA, Ni Y, Urban S. Hepatitis delta virus: insights into a peculiar pathogen and novel treatment options. Nat Rev Gastroenterol Hepatol 2016;13:580–589. [PubMed: 27534692]
4. Winer BY, Ploss A. Determinants of hepatitis B and delta virus host tropism. Curr Opin Virol 2015;13:109–116. [PubMed: 26164658]
5. Hetzel U, Szirovicza L, Smura T, Prahauser B, Vapalahti O, Kipar A, Hepojoki J. Identification of a Novel Deltavirus in Boa Constrictors. MBio 2019;10.
6. Wille M, Netter HJ, Littlejohn M, Yuen L, Shi M, Eden JS, Klaassen M, et al. A Divergent Hepatitis D-Like Agent in Birds. Viruses 2018;10.

7. Sells MA, Chen ML, Acs G. Production of hepatitis B virus particles in Hep G2 cells transfected with cloned hepatitis B virus DNA. Proc Natl Acad Sci U S A 1987;84:1005–1009. [PubMed: 3029758]
8. Gripon P, Rumin S, Urban S, Le Seyec J, Glaise D, Cannie I, Guyomard C, et al. Infection of a human hepatoma cell line by hepatitis B virus. Proc Natl Acad Sci U S A 2002;99:15655–15660. [PubMed: 12432097]
9. Ni Y, Lempp FA, Mehrle S, Nkongolo S, Kaufman C, Falth M, Stindt J, et al. Hepatitis B and D viruses exploit sodium taurocholate co-transporting polypeptide for species-specific entry into hepatocytes. Gastroenterology 2014;146:1070–1083. [PubMed: 24361467]
10. Gripon P, Diot C, Theze N, Fourel I, Loreal O, Brechot C, Guguen-Guillouzo C. Hepatitis B virus infection of adult human hepatocytes cultured in the presence of dimethyl sulfoxide. J Virol 1988;62:4136–4143. [PubMed: 3172341]
11. Ochiya T, Tsurimoto T, Ueda K, Okubo K, Shiozawa M, Matsubara K. An in vitro system for infection with hepatitis B virus that uses primary human fetal hepatocytes. Proc Natl Acad Sci U S A 1989;86:1875–1879. [PubMed: 2538818]
12. Galle PR, Hagelstein J, Kommerell B, Volkmann M, Schranz P, Zentgraf H. In vitro experimental infection of primary human hepatocytes with hepatitis B virus. Gastroenterology 1994;106:664–673. [PubMed: 8119538]
13. Zhou M, Zhao F, Li J, Cheng Z, Tian X, Zhi X, Huang Y, et al. Long-term maintenance of human fetal hepatocytes and prolonged susceptibility to HBV infection by co-culture with non-parenchymal cells. J Virol Methods 2014;195:185–193. [PubMed: 24134944]
14. Kidambi S, Yarmush RS, Novik E, Chao P, Yarmush ML, Nahmias Y. Oxygen-mediated enhancement of primary hepatocyte metabolism, functional polarization, gene expression, and drug clearance. Proc Natl Acad Sci U S A 2009;106:15714–15719. [PubMed: 19720996]
15. Ploss A, Khetani SR, Jones CT, Syder AJ, Trehan K, Gaysinskaya VA, Mu K, et al. Persistent hepatitis C virus infection in microscale primary human hepatocyte cultures. Proc Natl Acad Sci U S A 2010;107:3141–3145. [PubMed: 20133632]
16. March S, Ng S, Velmurugan S, Galstian A, Shan J, Logan DJ, Carpenter AE, et al. A Microscale Human Liver Platform that Supports the Hepatic Stages of Plasmodium falciparum and vivax. Cell Host Microbe 2013;14:104–115. [PubMed: 23870318]
17. Shlomai A, Schwartz RE, Ramanan V, Bhatta A, de Jong YP, Bhatia SN, Rice CM. Modeling host interactions with hepatitis B virus using primary and induced pluripotent stem cell-derived hepatocellular systems. Proc Natl Acad Sci U S A 2014;111:12193–12198. [PubMed: 25092305]
18. Ortega-Prieto AM, Skelton JK, Wai SN, Large E, Lussignol M, Vizcay-Barrena G, Hughes D, et al. 3D microfluidic liver cultures as a physiological preclinical tool for hepatitis B virus infection. Nat Commun 2018;9:682. [PubMed: 29445209]
19. Winer BY, Huang TS, Pludwinski E, Heller B, Wojcik F, Lipkowitz GE, Parekh A, et al. Long-term hepatitis B infection in a scalable hepatic co-culture system. Nat Commun 2017;8:125. [PubMed: 28743900]
20. Bonn B, Svanberg P, Janefeldt A, Hultman I, Grime K. Determination of Human Hepatocyte Intrinsic Clearance for Slowly Metabolized Compounds: Comparison of a Primary Hepatocyte/Stromal Cell Co-culture with Plated Primary Hepatocytes and HepaRG. Drug Metab Dispos 2016;44:527–533. [PubMed: 26851239]
21. Schulze A, Gripon P, Urban S. Hepatitis B virus infection initiates with a large surface protein-dependent binding to heparan sulfate proteoglycans. Hepatology 2007;46:1759–1768. [PubMed: 18046710]
22. Gudima S, He Y, Chai N, Bruss V, Urban S, Mason W, Taylor J. Primary human hepatocytes are susceptible to infection by hepatitis delta virus assembled with envelope proteins of woodchuck hepatitis virus. J Virol 2008;82:7276–7283. [PubMed: 18495772]
23. Winer BY, Shirvani-Dastgerdi E, Bram Y, Sellau J, Low BE, Johnson H, Huang T, et al. Preclinical assessment of antiviral combination therapy in a genetically humanized mouse model for hepatitis delta virus infection. Sci Transl Med 2018;10.

24. Frei AP, Bava FA, Zunder ER, Hsieh EW, Chen SY, Nolan GP, Gherardini PF. Highly multiplexed simultaneous detection of RNAs and proteins in single cells. Nat Methods 2016;13:269–275. [PubMed: 26808670]

25. Blank A, Markert C, Hohmann N, Carls A, Mikus G, Lehr T, Alexandrov A, et al. First-in-human application of the novel hepatitis B and hepatitis D virus entry inhibitor myrcludex B. J Hepatol 2016;65:483–489. [PubMed: 27132172]

26. Shan J, Schwartz RE, Ross NT, Logan DJ, Thomas D, Duncan SA, North TE, et al. Identification of small molecules for human hepatocyte expansion and iPS differentiation. Nat Chem Biol 2013;9:514–520. [PubMed: 23728495]

27. Smedile A, Farci P, Verme G, Caredda F, Cargnel A, Caporaso N, Dentico P, et al. Influence of delta infection on severity of hepatitis B. Lancet 1982;2:945–947. [PubMed: 6127458]

28. Krogsgaard K, Kryger P, Aldershvile J, Andersson P, Sorensen TI, Nielsen JO. Delta-infection and suppression of hepatitis B virus replication in chronic HBsAg carriers. Hepatology 1987;7:42–45. [PubMed: 3804204]

29. Zhang Z, Filzmayer C, Ni Y, Sultmann H, Mutz P, Hiet MS, Vondran FWR, et al. Hepatitis D virus replication is sensed by MDA5 and induces IFN-beta/lambda responses in hepatocytes. J Hepatol 2018;69:25–35. [PubMed: 29524530]

30. Lucifora J, Durantel D, Testoni B, Hantz O, Levrero M, Zoulim F. Control of hepatitis B virus replication by innate response of HepaRG cells. Hepatology 2010;51:63–72. [PubMed: 19877170]

31. Wieland S, Thimme R, Purcell RH, Chisari FV. Genomic analysis of the host response to hepatitis B virus infection. Proc Natl Acad Sci U S A 2004;101:6669–6674. [PubMed: 15100412]

32. Suslov A, Boldanova T, Wang X, Wieland S, Heim MH. Hepatitis B Virus Does Not Interfere with Innate Immune Responses in the Human Liver. Gastroenterology 2018.

33. Shi YX, Huang CJ, Yang ZG. Impact of hepatitis B virus infection on hepatic metabolic signaling pathway. World J Gastroenterol 2016;22:8161–8167. [PubMed: 27688657]

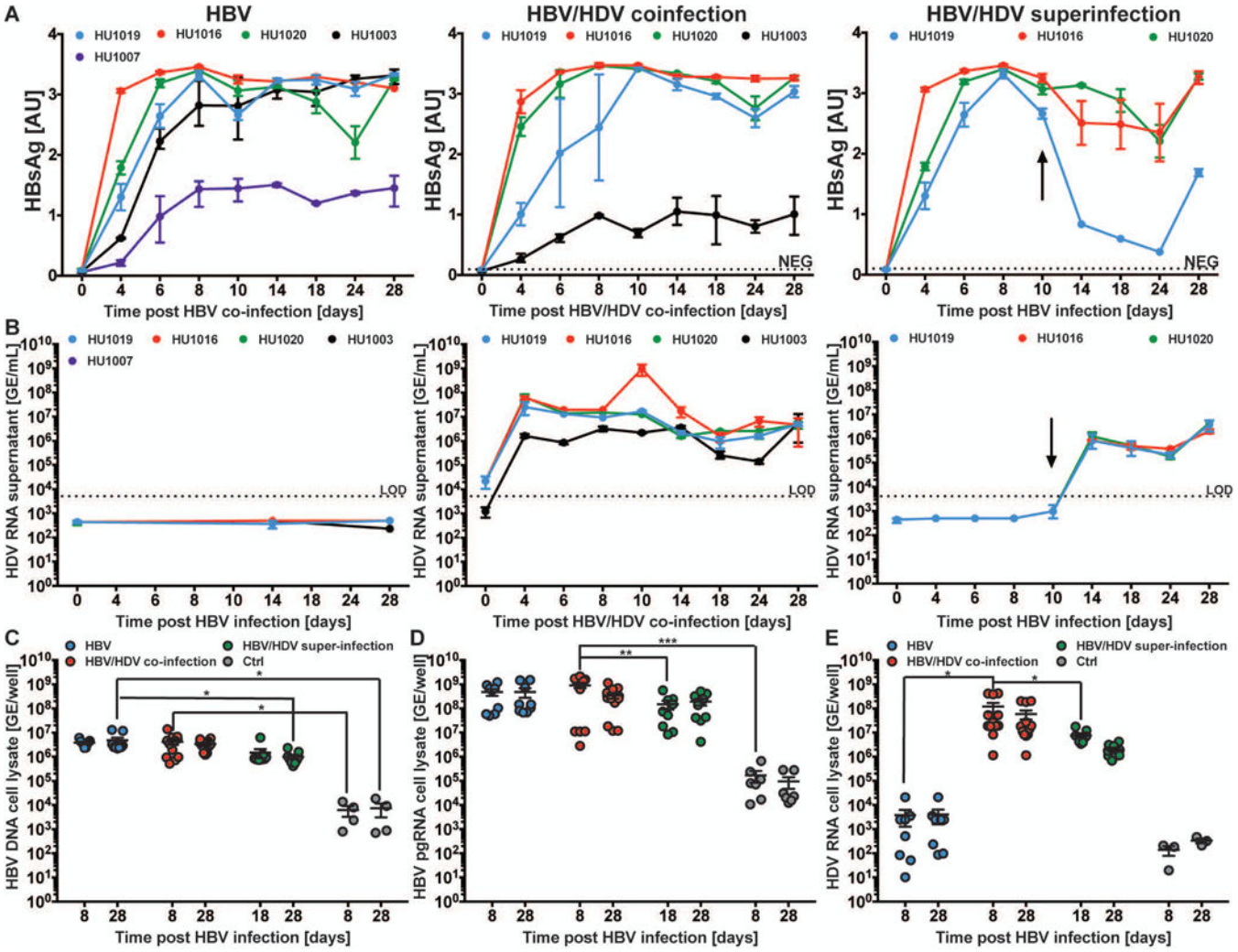

Fig. 1. HBV mono-infection, HBV/HDV co-infection, and HBV/HDV super-infection kinetics in SACC-PHHs.

SACC-PHHs were infected with either HBV, HBV/HDV (co-infection), or were first persistently infected with HBV and then with HDV (super-infection). (**A**) Longitudinal HBsAg ELISA data. (**B**) HDV RNA RT-qPCR data from supernatants. HBV DNA (**C**), HBV pgRNA (**D**), or HDV RNA **(E)** in the cell lysates. All data are presented as mean ± SEM. Statistical significance was determined using ANOVA. *P < 0.05, **P < 0.01, ***P < 0.001, and ****P < 0.0001.

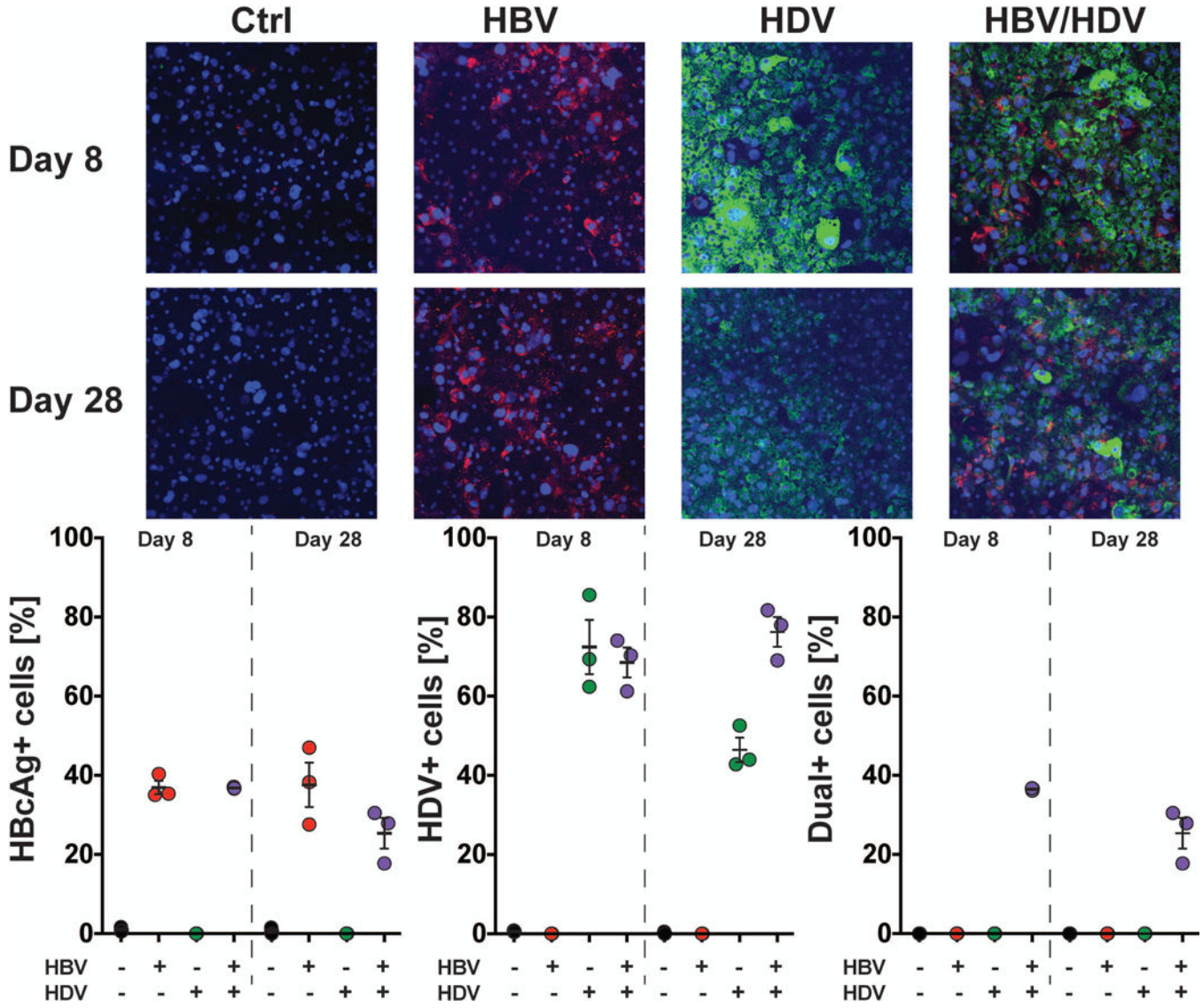

Fig. 2. Quantification of infection in HBV, HDV, and co-infected SACC-PHHs by HDV vPLAYR/TSA and anti-HBcAg immunofluorescence staining.

SACC-PHHs were either infected with HBV (MOI=4,000), HDV (MOI=1,000), or both HBV/HDV (HBV MOI=4,000, HDV MOI=1,000). (**A**) At 8 (top) and 28 (bottom) days post infection, control and infected SACC-PHHs were fixed and stained for HDV genomic RNA (green) by a vPLAYR/TSA procedure and for HBcAg (red) by an anti-HBcAg antibody as well as with DAPI (blue) for nuclear DNA. Quantification of three different images for each experimental condition were performed (approximately ~800 cells total per condition) for (**B**) HBcAg positive cells; (**C**) HDV genomic RNA positive cells; and (**D**) dual-positive cells.

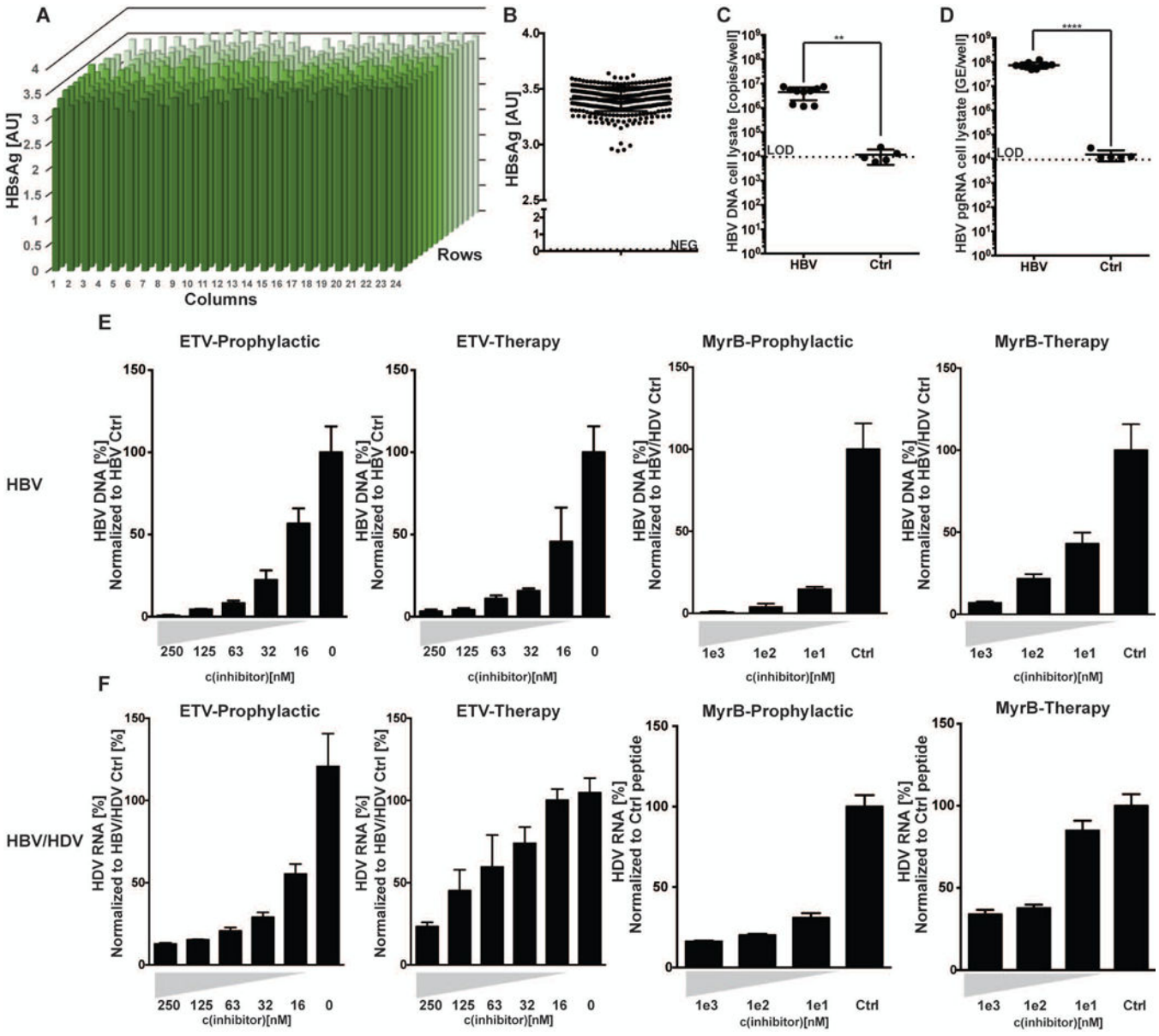

Fig. 3. Assessment of clinically relevant drug treatments for HBV mono-infection and HBV/HDV co-infection of SACC-PHHs in a 384 well microwell format.

(**A**) SACC-PHHs in a 384 well format were infected with HBV and viremia assessed for each well by HBsAg ELISA. (**B**) Summary of HBsAg concentrations determined across plate shown in (**A**). Coefficient of variance across the 384 well plate equaled 3.2%. HBV DNA **(C)** and HBV pgRNA **(D)** from cell lysates of HBV infected vs control cultures as assessed by qPCR (HBV n=10; control n=5). For panel (**E**), SACC-PHHs were challenged with HBV. The x-axis equals drug concentration and the y-axis the amount of HBV DNA (for ETV) or HBsAg secretion (for MyrB) normalized to untreated, HBVcc-infected untreated control cells or HBVcc-infected cells treated with a control peptide, respectively. For panels (**F**) SACC-PHHs were co-infected with HBV/HDV and HDV RNA was quantified by RT-qPCR in supernatant (**far left**) and cell lysate (**second from left**). Co-

infected SACC-PHHs were treated with the entry inhibitor MyrB prophylactically (**second from right**) or therapeutically (**far right**), with the x axis showing drug concentration and the y axis the amount of HDV RNA present in the supernatant normalized to that secreted by co-infected cells treated with a control peptide. All data are presented as mean ± SEM. Statistical significance was determined using ANOVA. *P < 0.05, **P < 0.01, ***P < 0.001, and ****P < 0.0001.

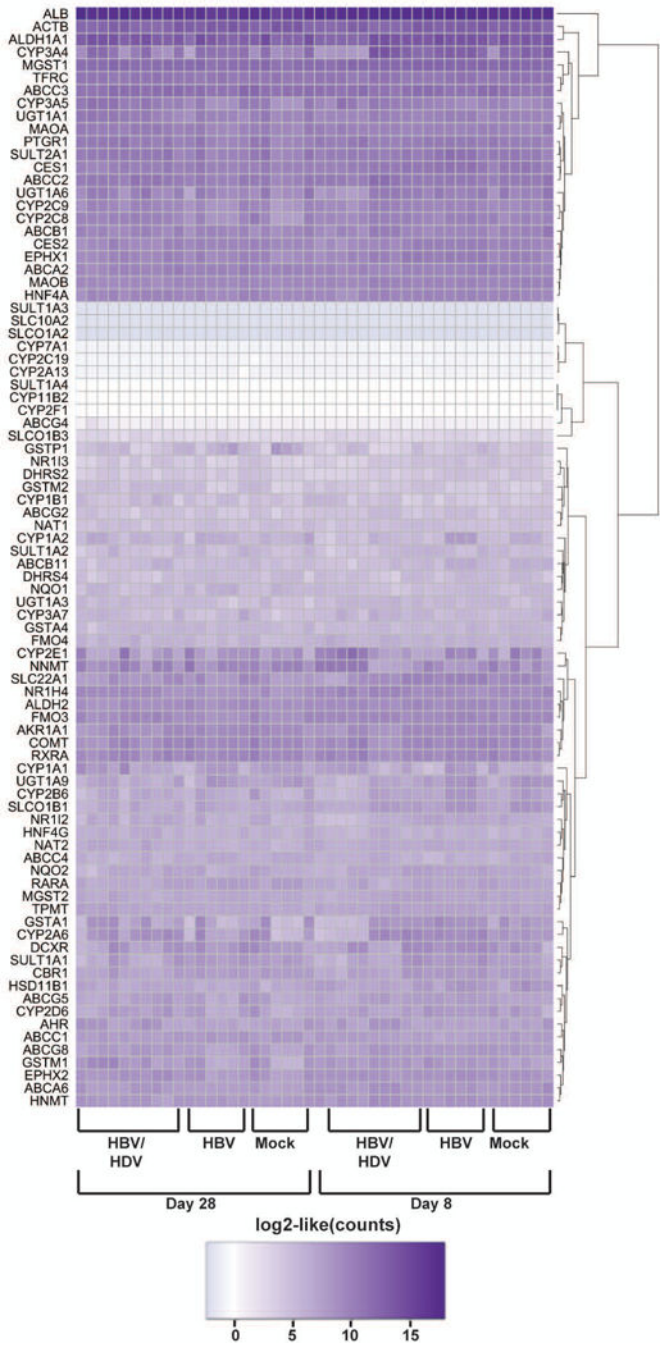

Fig. 4. Regardless of experimental condition, minimal variation observed for 86 drug-metabolizing, liver-specific transcripts, in SACC-PHHs.

Regularized log2 transformed (rlog function in DESeq2) RNAseq counts from SACC-PHHs mono-infected with HBV, co-infected with HBV/HDV or mock-infected for 86 drug-metabolizing enzymes, predominantly regulated at the transcriptional level and expressed by the human liver, are shown.

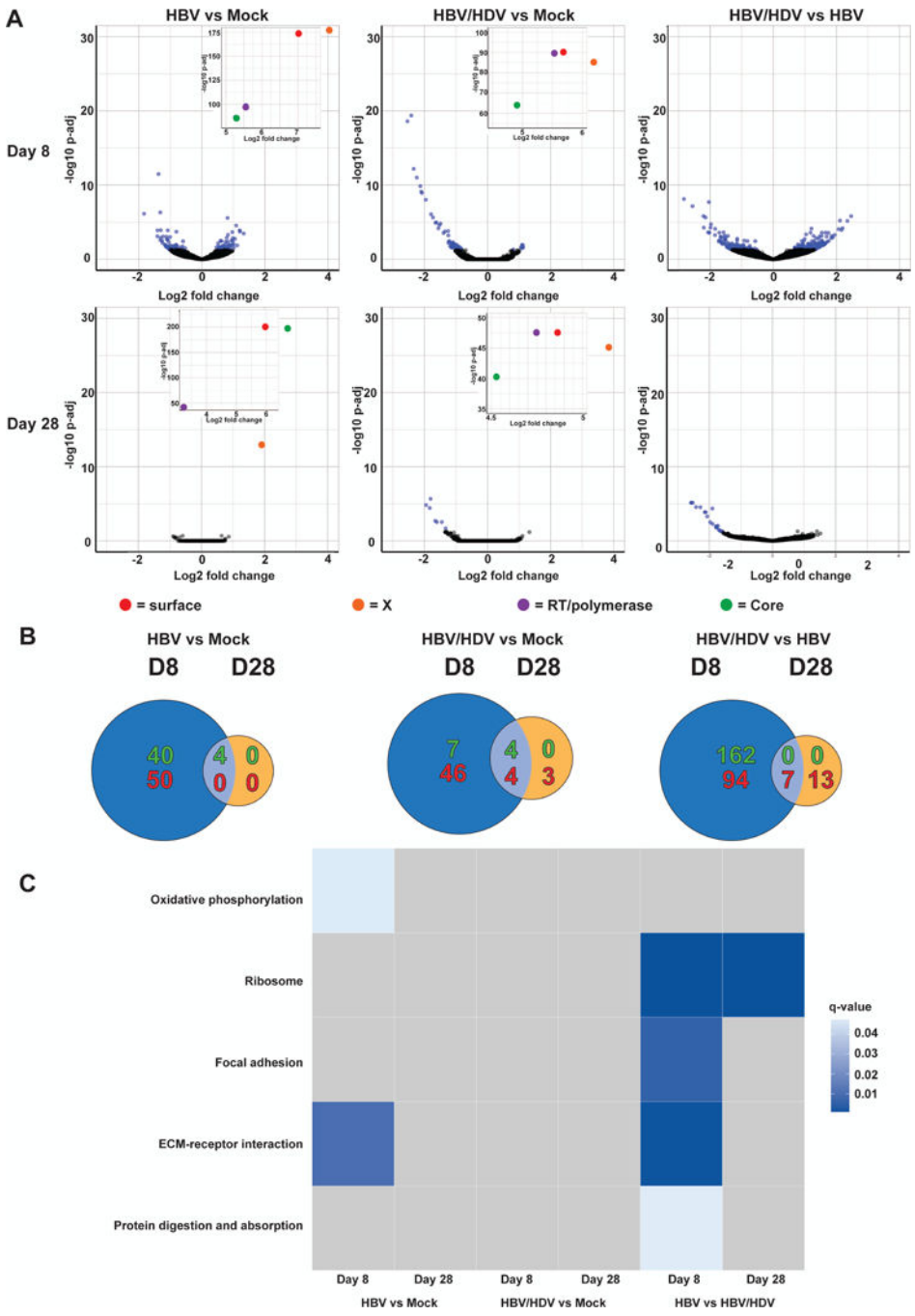

Fig. 5. Transcriptomic analysis of "early" and "late" stage of HBV mono-infected and HBV/HDV co-infected SACC-PHHs.

RNA was isolated at 8 and 28 dpi from SACC-PHHs HBV mono-, HBV/HDV co- or mock-infected. A cDNA library was then generated and sequenced. (**A**) Volcano plots of differentially expressed genes in mono-infected vs mock, co-infected vs mock, or co- vs mono-infected at 8 dpi (top row) and 28 dpi (bottom row). Each point represents a gene, with those having a $p_{adj} \leq 0.05$ colored blue and those with a $p_{adj} > 0.05$ colored black. HBV genes are indicated in red, orange, purple or green. (**B**) Venn diagram of genes up- (shown in

green) or down-regulated (shown in red) between mono-infected vs mock, co-infected vs mock, and co- vs mono-infected at 8 and 28 dpi. Genes were considered up- or down-regulated if the absolute value of $\log_2$(fold change) ≥ 0.5 and $p_{adj} \leq 0.05$. (**C**) Significantly enriched pathways (q-value ≥ 0.07) determined using GAGE comparing mono-infected vs control, co-infected vs control, and co- vs mono-infected at 8 and 28 dpi.

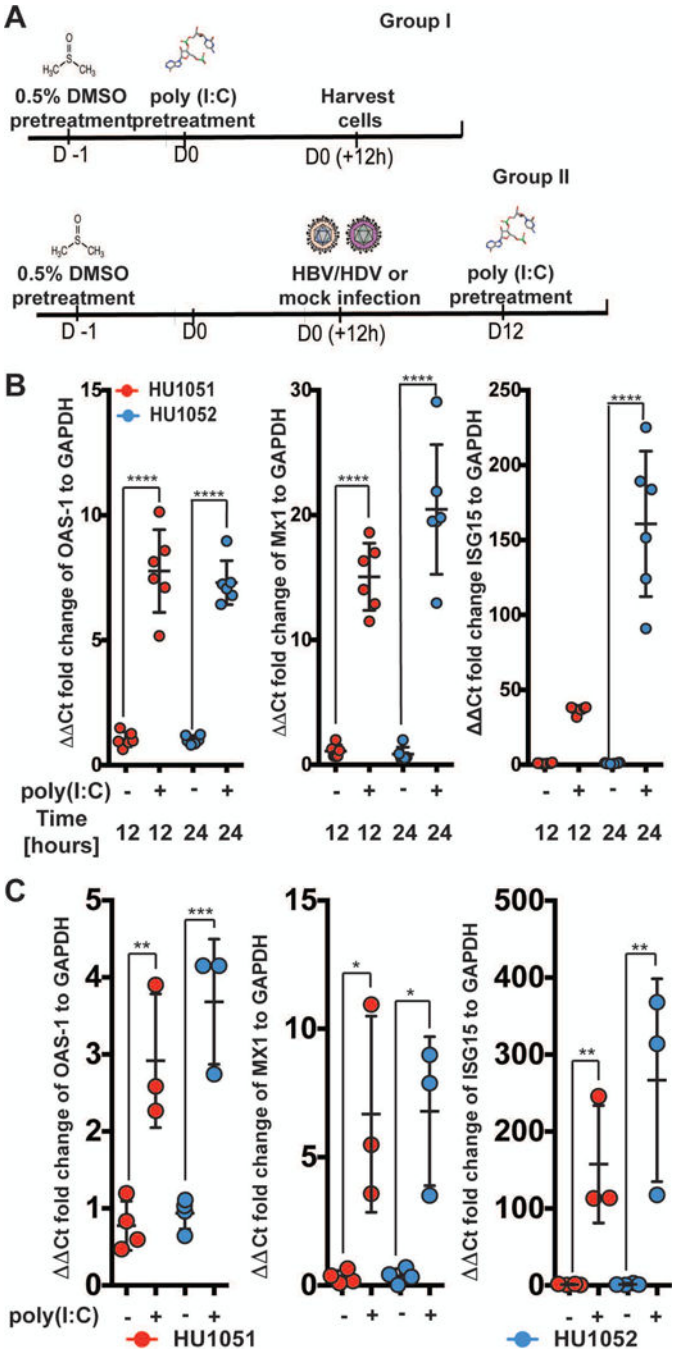

Fig. 6: HBV/HDV co-infection does not generally impair cell-intrinsic innate defenses.

(A) Schematic of experimental time course **(B)** Fold increase in the ISGs OAS-1 (**left**), MX1 (**middle**) and ISG15 (**right**) normalized to GAPDH, 12 and 24 hours post poly(I:C) transfection, quantified by RT-qPCR in the absence of infection. (**C**) Analysis of OAS-1 **(left),** MX1 (**middle**), and ISG15 (**right**) mRNA expression 12 hours post poly(I:C) exposure of SACC-PHHs co-infected 12 days prior. Different colors represent indicated hepatocyte donors. All data are presented as mean ± SEM. Statistical significance was

determined using ANOVA. *P < 0.05, **P < 0.01, ***P < 0.001, and ****P < 0.0001.
Abbreviations: GAPDH, glyceraldehyde 3-phosphate dehydrogenase.

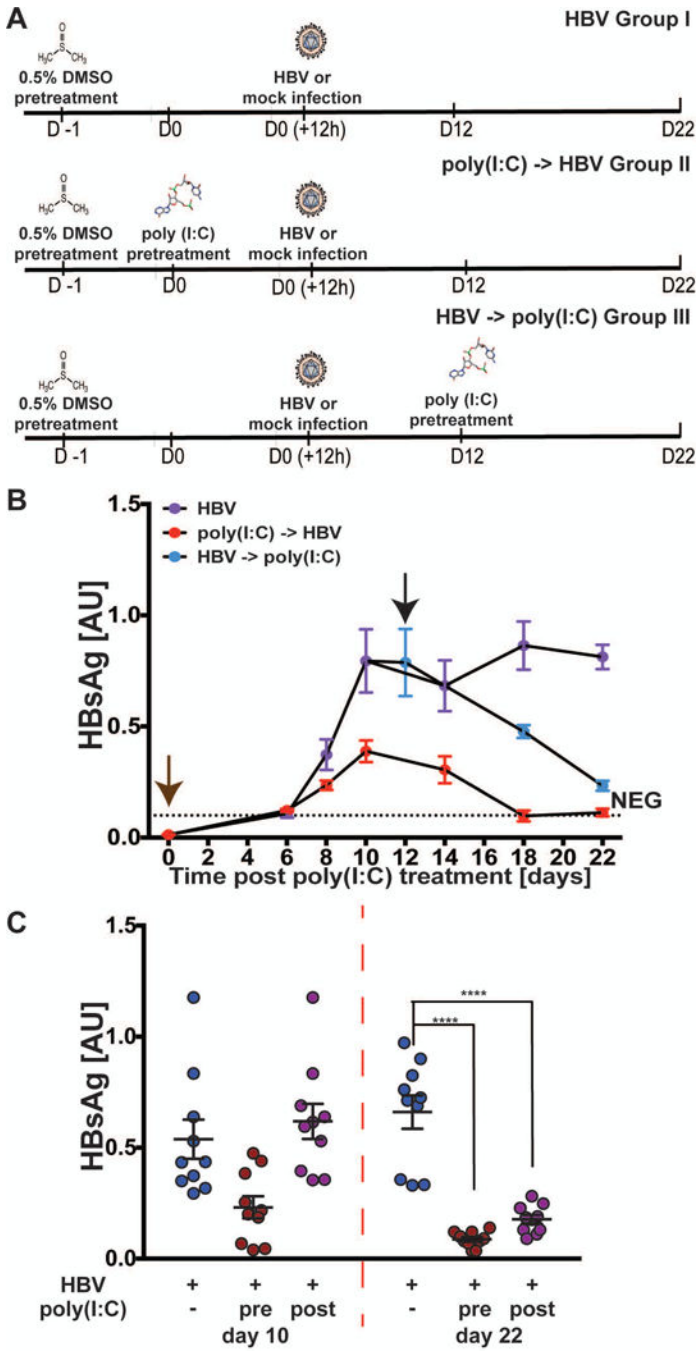

Fig. 7: Induction of innate immunity by poly(I:C) treatment leads to suppression of HBV.

(**A**) Schematic of experimental time course for poly(I:C)-transfected SACC-PHHs infected with HBV. Longitudinal measurements of HBsAg by ELISA in supernatants (**B-C**) of SACC-PHHs +/− poly(I:C) as shown in panel **A.** Brown and black arrows indicate poly(I:C) transfection either pre- or post-establishment of persistent infection, respectively. Co-infected SACC-PHHs +/− poly(I:C) were lysed 12 and 22 dpi. A separate set of pre-infected SACC-PHHs for each donor were also lysed. Statistical significance was determined using ANOVA. ****P < 0.0001.

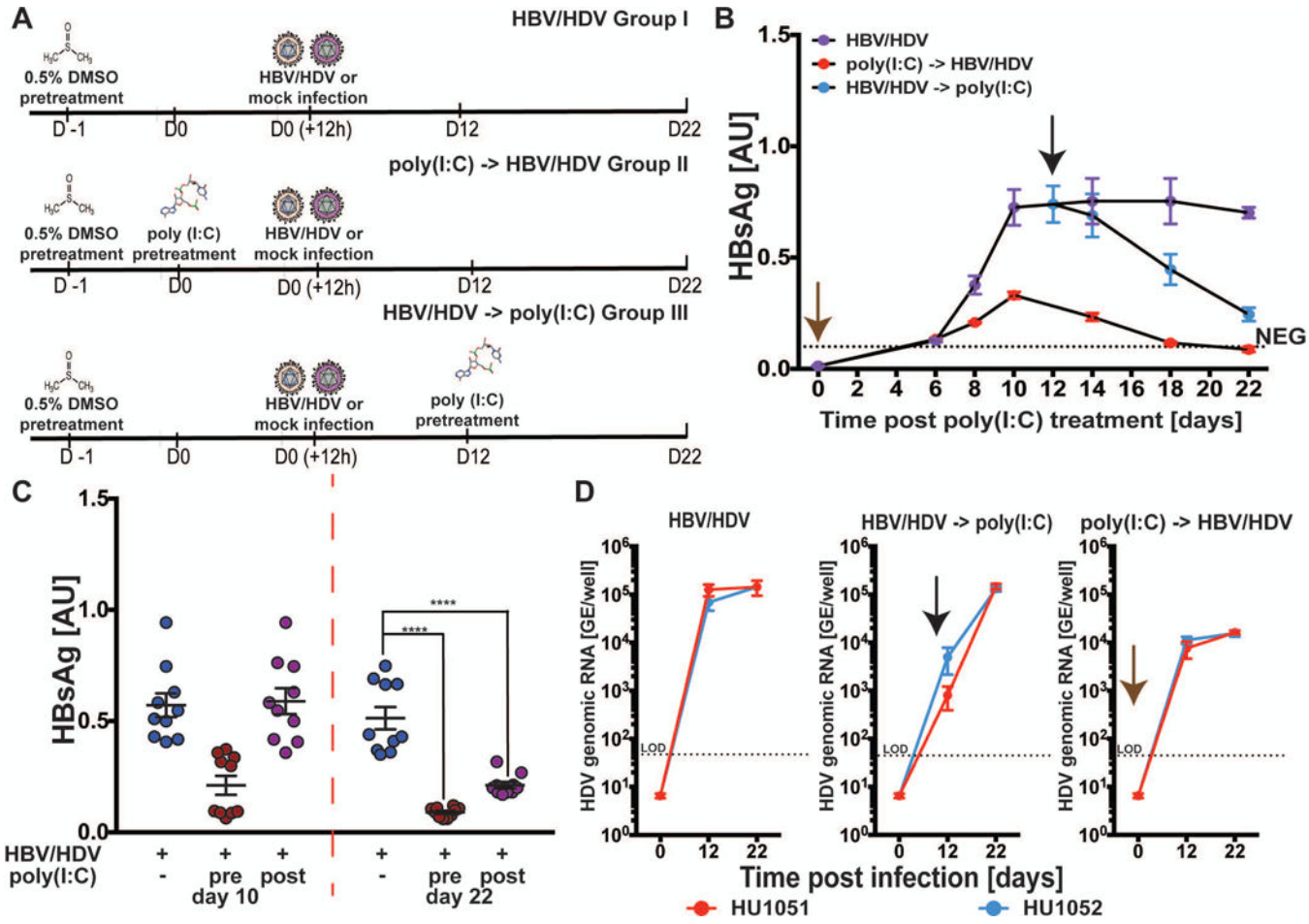

Fig. 8: Induction of innate immunity has little effect on HDV infection.

(**A**) Schematic of experimental time course for poly(I:C)-transfected SACC-PHHs co-infected with HBV/HDV. Longitudinal measurements of HBsAg by ELISA in supernatants of co-infected (**B-C**) SACC-PHHs +/− poly(I:C) as shown in panel **A**. Brown and black arrows indicate poly(I:C) transfection either pre- or post-establishment of persistent infection, respectively. Co-infected SACC-PHHs +/− poly(I:C) were lysed 12 and 22 dpi. A separate set of pre-infected SACC-PHHs for each donor were also lysed. (**D**) Quantification of intracellular HDV genomic RNA by RT-qPCR at 12 and 22 dpi in cultures mock treated (**left**), or exposed to poly(I:C) post- (**middle**) or pre- (**right**) infection. Statistical significance was determined using ANOVA. ****P < 0.0001.